

Enterohepatic recirculation model of irinotecan (CPT-11) and metabolite pharmacokinetics in patients with glioma

Islam R. Younis · Samuel Malone · Henry S. Friedman ·
Larry J. Schaaf · William P. Petros

Received: 5 July 2007 / Accepted: 2 May 2008 / Published online: 22 May 2008
© Springer-Verlag 2008

Abstract

Background Enterohepatic recirculation of irinotecan and one of its metabolites, SN-38, has been observed in pharmacokinetic data sets from previous studies. A mathematical model that can incorporate this phenomenon was developed to describe the pharmacokinetics of irinotecan and its metabolites.

Patients and methods A total of 32 patients with recurrent malignant glioma were treated with weekly intravenous administration of irinotecan at a dose of 125 mg/m². Plasma concentrations of irinotecan and its three major metabolites were determined. Pharmacokinetic models were developed and tested for simultaneous fit of parent drug and metabolites, including a recirculation component.

Results Rebound in the plasma concentration suggestive of enterohepatic recirculation at approximately 0.5–1 h post-infusion was observed in most irinotecan plasma concentration profiles, and in some plasma profiles of the SN-38 metabolite. A multi-compartment model containing a

recirculation chain was developed to describe this process. The recirculation model was optimal in 22 of the 32 patients compared to the traditional model without the recirculation component.

Conclusion A recirculation chain incorporated in a multi-compartment pharmacokinetic model of irinotecan and its metabolites appears to improve characterization of this drug's disposition in patients with glioma.

Keywords Irinotecan · Pharmacokinetics · Enterohepatic recirculation

Introduction

Irinotecan (CPT-11; Camptosar[®]) is used in the treatment of a variety of malignancies such as ovarian [1, 2], and colorectal cancers [3, 4]. More recently, it has shown activity in the treatment of glioma [5].

Both hydrolysis and metabolism are responsible for elimination of irinotecan (Fig. 1). The hydrolysis pathway is catalyzed by carboxy esterases and results in the formation of the active metabolite 7-ethyl-10-hydroxycamptothecin (SN-38). Although both human carboxy esterase isoenzymes 1 and 2 were identified to be involved in this biotransformation, human carboxy esterase 2 appears to play a more important role in cancer patients [6, 7]. SN-38 is further metabolized in human liver by UDP-glucuronosyl transferase 1A1 to the inactive metabolite 7-ethyl-10-[3,4,5-trihydroxy-pyran-2-carboxylic acid]-camptothecin (SN-38G) [8, 9]. SN-38 levels are about 100-fold lower than that of irinotecan, with elimination half-life of approximately 10.2 h [10]. SN-38 glucuronide is present in plasma at higher concentrations than SN-38 [11]. The metabolic biotransformation of irinotecan is catalyzed by CYP450 3A4. The major metabolites formed

I. R. Younis · W. P. Petros (✉)
Department of Basic Pharmaceutical Sciences
and Mary Babb Randolph Cancer Center,
West Virginia University Health Sciences Center,
P.O. Box 9300, Morgantown, WV 26506, USA
e-mail: wpetros@hsc.wvu.edu

S. Malone · H. S. Friedman
Duke University Medical Center, Durham, NC, USA

H. S. Friedman
Department of Surgery,
Duke University Medical Center, Durham, NC, USA

L. J. Schaaf
The Ohio State University Comprehensive Cancer Center,
Columbus, OH, USA

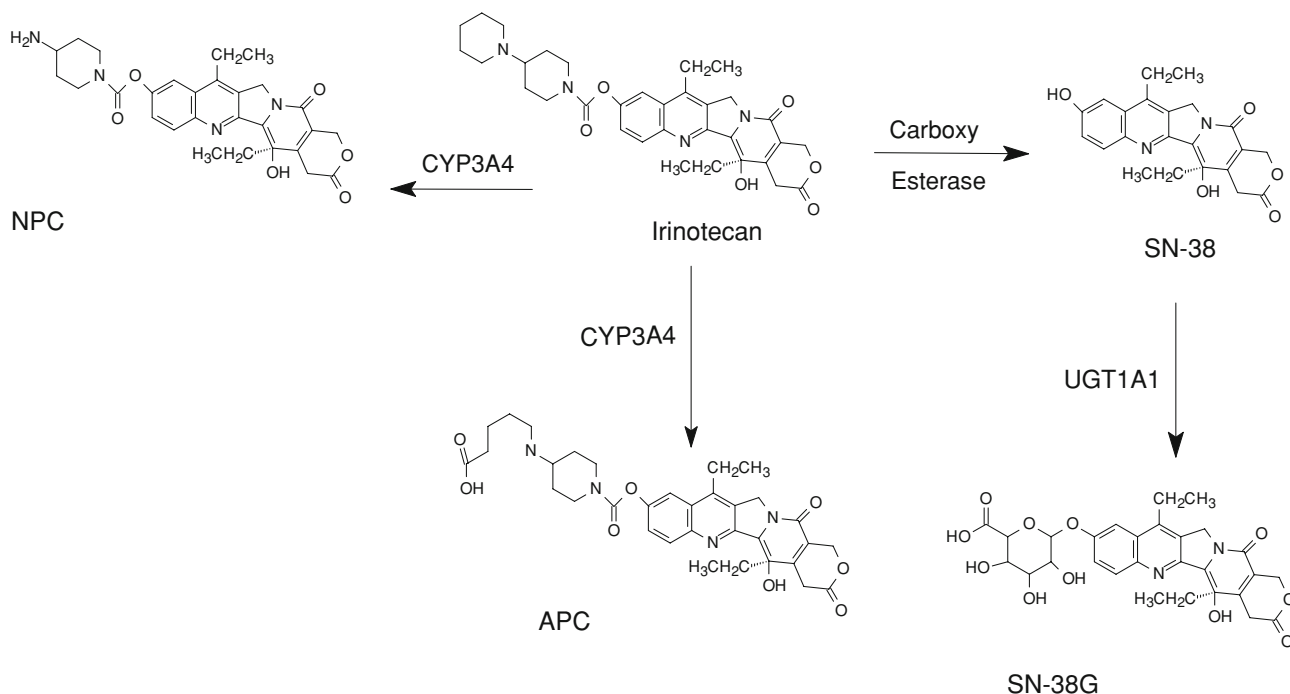


Fig. 1 Metabolic scheme of irinotecan

through this pathway are 7-ethyl-10-[4-N-(5-aminopentanoic acid)-1-piperidino]-1-amino]-carbonyloxycamptothecin (APC) and 7-ethyl-10-[4-(1-piperidino)-1-amino]-carbonyloxycamptothecin (NPC) [12]. Only small fractions of irinotecan and its metabolites are eliminated in urine and a higher proportion in the bile.

An apparent enterohepatic recirculation of irinotecan and SN-38 is evident by the rebound in plasma levels at about 0.5–1.0 h following intravenous infusion [13]. We particularly noted this effect in some patients receiving concomitant anticonvulsant medications, however no formal pharmacokinetic model has been published which could describe this complex process in the context of metabolite pharmacokinetics [14].

The pharmacokinetics of irinotecan display high inter-patient variation and are typically described by two or three compartment, first order models [15]. We attempted to utilize such models to evaluate parent drug and metabolites in a population of patients with brain tumors, many of which were receiving metabolic enzyme-inducing anticonvulsants [14]. Observable delayed (post-infusion) increases in plasma irinotecan (and to some degree, SN-38) led us to explore alternative approaches for mathematical description of these data. This paper reports use of our published irinotecan pharmacokinetic data to develop a novel enterohepatic recirculation model which incorporates multiple metabolite information. In addition, we have provided data on an additional metabolite (APC) which was not available at the time of the previous publication.

Patients and methods

Inclusion criteria

Patients older than 18 years of age, diagnosed with recurrent primary malignant glioma [glioblastoma multiforme, anaplastic astrocytoma (AA), or anaplastic oligodendroglioma (AO)] and exhibiting a Karnofsky performance status $\geq 60\%$ were included in this pharmacokinetic study. Other pertinent eligibility criteria included adequate renal function (serum creatinine ≤ 1.5 mg/dL), adequate hepatic function (blood nitrogen level < 25 mg/dL, serum AST and bilirubin levels $< 1.5 \times$ upper limit of normal), and adequate bone marrow function (hematocrit concentration $> 29\%$, absolute neutrophil count $> 1,500$ cell/ μ L, platelet count $> 125,000$ cells/ μ L). Patients who were receiving corticosteroids were required to be on a stable dose for 2 weeks prior to treatment.

Written informed consent was obtained from patients according to the guidelines of the institutional review board prior to initiation of the study. Additional details of the patient eligibility criteria are included elsewhere [14].

Treatment

Irinotecan was diluted with 500 mL of 5% dextrose solution, and administered by a 90 min IV infusion once weekly for 4 weeks, followed by 2 weeks rest. The starting dose of irinotecan was 125 mg/m^2 for all patients. Irinotecan was

obtained from the Cancer Therapy Evaluation Program of the National Cancer Institute (NCI) as a sterile solution of 20 mg/mL in 2- or 5-mL vials.

Standard doses of ondansetron and an IV bolus dose of dexamethasone (10–20 mg) were administered before each irinotecan dose to prevent emesis. Patients who exhibited cholinergic affects with 2.5 h of starting of irinotecan infusion were treated with atropine (1 mg, IV). Patients who had late diarrhea were treated with loperamide. Patients already taking anticonvulsants continued treatment as prescribed. Chronic oral administration of corticosteroids was used to reduce tumor produced effects.

Pharmacokinetic studies

Pharmacokinetics of irinotecan and its metabolites, SN-38, SN38-G, and APC were conducted during, and up to 24 h after the first irinotecan infusion. Blood samples (5 mL) were drawn into heparinized tubes before irinotecan infusion at 30, 60, and 90 min (end of infusion), and at 5, 15, and 30 min and 1, 2, 4, 6, 8, and 24 h following the completion of the infusion. Blood samples were immediately placed into slurry of ice and water. Plasma was separated, as soon as possible, by centrifugation at 1,000–1,200×g (3,000 rpm) for 20 min, and stored at -70°C until analyzed.

Plasma concentrations of irinotecan and its metabolites (SN-38, SN-38G and APC) were determined using a validated, sensitive, and specific high performance liquid chromatography with fluorescence detection as described previously [14]. The lower limits of quantification were 1.3, 0.5, and 1.0 ng/mL for irinotecan, SN-38, and APC, respectively. Intra- and inter-variability in the assay method was <10% for each analyte.

Pharmacokinetic data analysis

Pharmacokinetic analyses were performed using non-compartmental as well as compartmental pharmacokinetic modeling. Initial parameters were determined by generalized least-square regression of plasma concentration time points, as implemented by the ADAPT program (Biomedical Simulations Resource, University of Southern California) [16]. Irinotecan and its metabolite data were then evaluated by ADAPT using a nonlinear, open, multi-compartment pharmacokinetic model. The model included two compartments for irinotecan, and one compartment each for SN-38 and APC. The data were also evaluated using a model that takes into account the phenomenon of enterohepatic recirculation. This model additionally incorporated a recirculation “chain” stemming off of the irinotecan compartment and leading back into it as depicted in Fig. 2. The recirculation chain consisted of five compartments, each of fixed

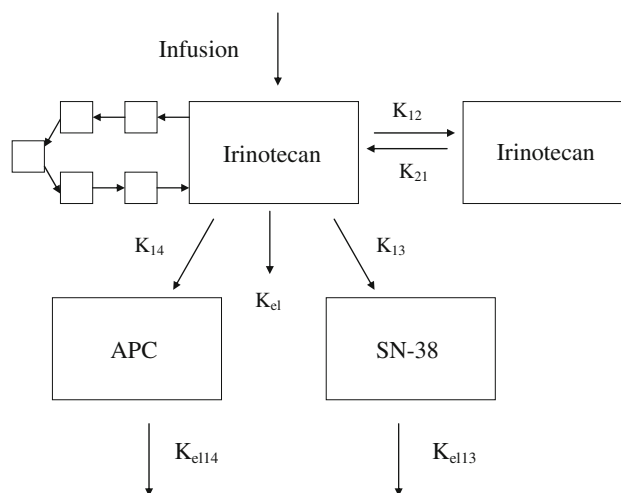


Fig. 2 The enterohepatic recirculation model consists of irinotecan central compartment, irinotecan peripheral compartment, and SN-38 and APC plasma compartments, and the recirculation chain that consists of five compartments each of fixed volume

volume, with a single rate parameter that is equal to the rate constant of flow between each compartment in the chain. This rate parameter also determined the linear rate constants between the primary compartment and the chain compartment, and between the last chain compartment and the primary compartment. The virtue of having a single parameter is that it allows us to model the recirculation effects while adding minimum complexity to the model. To determine the best number of compartments in the model (five), we ran several informal trials on patients which appeared to display a high qualitative level of recirculation. A four compartment chain worked fairly well for some sets, and our decision to use five reflected our sense that a five compartment chain produced the best fit for the majority of recirculation sets. It should be noted that the five compartments in the chain do not represent any physiological compartment.

A metabolic ratio, estimated as the ratio of each metabolite to irinotecan (AUC_{0-24}), was used to measure the relative ratio of irinotecan conversion to SN-38, SN38 to SN-38G, and irinotecan metabolism to APC.

Model selection

The Akaike Information Criterion (AIC) was utilized to select the best model for each patient data set [17]. Four representative patients were utilized for the determination of appropriate weighing scheme for the analytes. A weighing scheme was selected before running both models. Initially we found that a scheme with a coefficient of 1 for irinotecan, 30 for SN-38, and 5 for APC produced the lowest SSR on average for the patients tested. Improvement in the scheme was evident when coefficients of 1 for irino-

tecan, 10 for SN-38, and 5 for APC were employed. Like the 1, 30, 5 scheme, the latter scheme produced relatively low SSR for the four representative patients, and the two schemes gave comparable results. In addition, the 1, 10, 5 scheme was chosen because the weights are in keeping with the fact that SN-38 is 10–1,000 times more active than irinotecan, and the activity of APC falls between that of irinotecan and SN-38. Although we experimented with weighting schemes such as 1, 135, 3.5, which is more in line with the relative magnitudes of the analyte activity levels (and which makes the weighted SSR the same order of magnitude for each of the analytes), schemes that gave higher weight to SN-38 inevitably yielded higher total SSRs. Qualitatively, there seemed to be a trade off in some cases between fitting irinotecan well and fitting SN-38 well. In addition, weighting schemes that fit irinotecan well also seemed to fit APC well. After deciding on a weighting scheme, we estimated parameters for each patient using both the standard model and the recirculation model.

The best fit model was selected on a per-patient basis, using analyses of each patient with the recirculation model and the standard four compartment model. In the initial round of inspection, the model corresponding to the lower AIC value was termed the best model. In the second round of inspection, the data set of each patient was rated on a three point scale for the presence of enterohepatic recirculation, a subjective rating of 0, 1, or 2 was assigned to patients of they showed no, possible, or strong recirculation, respectively. This was done via a visual appraisal of the irinotecan and SN-38 concentration-time curves. If the standard model had been selected as best for a patient with a high qualitative degree of recirculation, the data set for that patient was rerun with alternative initial parameter estimates and the best model assignments were then finalized.

Results

Blood samples from 32 patients, 20 males and 12 females, were analyzed for irinotecan, SN-38, SN-38G, and APC. All patients received 125 mg/m² of irinotecan. Most of the patients ($n = 29$) were initially diagnosed with glioblastoma multiforme (GBM), two with AA, and one with AO. All the patients except two received enzyme inducing antiepileptic drug treatment.

Pharmacokinetic variables for irinotecan and its metabolites were determined from concentration-time data using non-compartmental and compartmental analysis. Figure 3 shows the plasma concentration-time curve of irinotecan, SN-38, and APC from a representative patient with an apparent recirculation profile. The plasma disposition curves for irinotecan were biphasic, with rapid decrease after the end of the infusion. The descent of the concentration-time

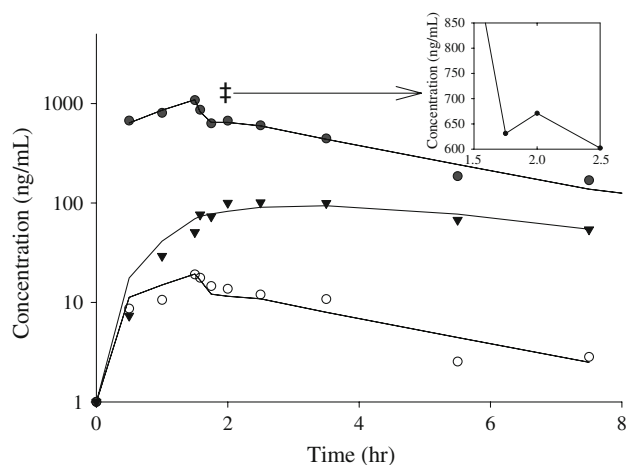


Fig. 3 Plasma concentration-time profile, in a representative patient of enterohepatic recirculation, for irinotecan (*filled circle*), SN-38 (*open circle*), and APC (*inverted triangle*). Irinotecan *double dagger* secondary peak after the end of the infusion indicative of enterohepatic recirculation. *Symbols* represent measured plasma concentration, and *solid lines* are obtained from predicted concentrations using the recirculation model connected point by point

curve following the end of infusion was interrupted by a brief upturn before continuing its fall in 22 patients, suggestive of an enterohepatic recirculation pathway. Plasma concentrations of APC displayed first order elimination. Figure 4 depicts the plasma concentration-time curve for irinotecan, SN-38, and APC in a patient with no enterohepatic recirculation. Irinotecan showed a rapid decay after the end of the infusion, with no upturn in irinotecan concentration following the end of the infusion. Table 1 shows the non-compartmental pharmacokinetic parameters for irinotecan, APC, SN-38, SN-38G. The mean \pm SD (ng/mL h) AUC_{0–24}

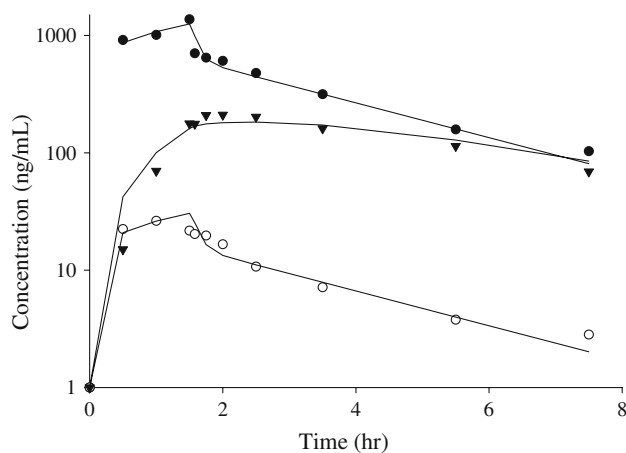


Fig. 4 Plasma concentration-time profile, in a representative patient of with no evidence of enterohepatic recirculation, for irinotecan (*filled circle*), SN-38 (*open circle*), and APC (*inverted triangle*). *Symbols* represent measured plasma concentration, and *solid lines* are obtained from point by point connection of the predicted plasma concentrations by the standard model

Table 1 Comparison of pharmacokinetic parameters for APC, irinotecan, SN-38, and SN-38G using non-compartmental analysis

	APC	Irinotecan	SN-38	SN-38G
Tmax (h)	2.31 ± 0.56	1.3 ± 0.3	1.2 ± 0.4	1.66 ± 0.28
Cmax (ng/mL)	178.6 ± 94.5	1,465 ± 598	12.9 ± 5.5	65.3 ± 25.7
Half-life (h)	5.5 ± 1.08	5.3 ± 0.86	8.5 ± 6.4	10.0 ± 2.9
AUC _{0–24} (ng h/mL)	1,337 ± 506	4,303 ± 1,321	63.9 ± 39.7	359 ± 157
AUC _{0–inf} (ng h/mL)	1,423 ± 565	4430 ± 1306	76.7 ± 50.5	440 ± 197
AUC % extrapolated	5.7 ± 5.0	3.1 ± 3.2	19.8 ± 11.1	16.7 ± 9.5

were $4,430 \pm 1,306$ for irinotecan, $1,337 \pm 506$ for APC, 63.9 ± 39.7 for SN-38, and 359 ± 157 for SN-38G. The AUC_{0–24} accounted for more than 95% of AUC_{0–inf} for irinotecan in all patients. AUC_{0–24} accounted for more than 70% of AUC_{0–inf} in 94, 87, and 100% of the patients for APC, SN-38G, and SN-38, respectively.

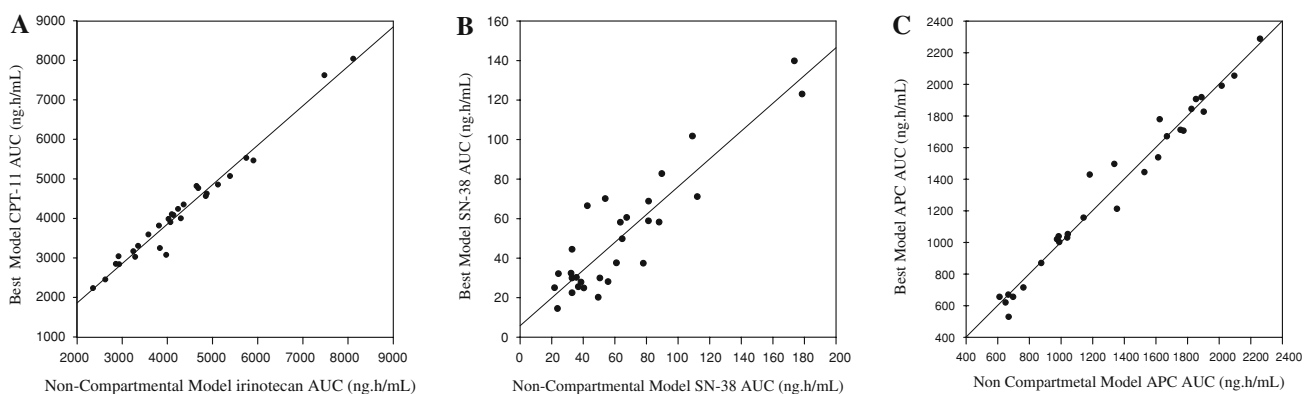
The relationship between irinotecan and its metabolites was evaluated by comparing the AUCs. The mean ± SD of the conversion of irinotecan to SN-38 was 0.016 ± 0.007 , while that of the metabolism of irinotecan to APC was 0.3 ± 0.1 . The mean ± SD for the conversion of SN-38 to SN-38G was 6.94 ± 3.09 .

The best fit model was selected on a per-patient basis, using analyses of each patient with the recirculation model and the standard four compartment model. The final parameters for the best and standard model are shown in Table 2. The recirculation model was best in 22 patients out of the 32 patient data sets, while the standard model was best in 10 patients. Figure 5 shows the relationship between the best model AUC for each analyte to the actual trapezoidal AUC. The regression produced R^2 of 0.971, 0.815, and 0.974 for irinotecan, SN-38, and APC, respectively. The mean precision error (MPE) and root mean squared error (RMSE) were used to quantify the degree of bias and preci-

Table 2 Final pharmacokinetic parameters for both the standard and recirculation model

	$V_{\text{IRINOTECAN}}$ (L/m ²)	K_{12} (h ⁻¹)	K_{21} (h ⁻¹)	K_{e1} (h ⁻¹)	K_{13} (h ⁻¹)	K_{e13} (h ⁻¹)	$V_{\text{SN-38}}$ (L/m ²)	K_{14} (h ⁻¹)	K_{e14} (h ⁻¹)	V_{APC} (L/m ²)
Standard model group ($n = 10$)										
Mean	24.70	38.25	6.66	6.27	2.55	123.69	394.39	1.14	0.41	40.68
Median	5.42	19.26	1.08	3.83	0.22	15.16	12.28	0.06	0.36	1.45
SD	42.50	58.87	18.29	8.36	6.82	282.12	1165.40	3.07	0.17	72.38
Range	0.77–133.40	0.36–197.70	0.01–58.71	0.00–26.82	0.01–21.90	0.18–905.17	0.50–3710.00	0.00–9.83	0.19–0.67	0.00–209.80
Recirculation model group ($n = 22$)										
Mean	8.60	6.52	0.55	5.12	0.29	17.30	19.19	0.31	0.44	14.31
Median	8.66	3.22	0.26	4.27	0.11	10.61	8.12	0.08	0.40	4.30
SD	4.60	8.10	0.70	4.45	0.63	25.43	34.40	0.69	0.16	30.76
Range	1.57–16.41	0.03–36.91	0.00–2.77	0.02–19.06	0.00–2.95	0.52–123.20	0.00–164.53	0.00–3.13	0.19–0.84	0.00–146.50

Out of 32 total patients, the standard model was designated as the optimal model for 10 patients and the recirculation model was designated the optimal model for the remaining 22

**Fig. 5** Linear regression of the optimal non-compartmental AUCs on the compartmental AUCs for irinotecan (a), SN-38 (b), and APC (c)

sion of the predicted AUC values. The MPE values for irinotecan, SN-38, and APC were -137 , -13.2 , and 1.09 , respectively. The RMSE values, which measure precision, were 249 , 20.82 , and 77.95 for irinotecan, SN-38, and APC, respectively.

Discussion

The importance of irinotecan as a chemotherapeutic agent is well established, however approaches to model its plasma disposition and complex metabolite profile are suboptimal for some patients in whom observable enterohepatic recirculation is evident. To our knowledge, this is the first report to incorporate the phenomena of enterohepatic circulation in the pharmacokinetic model used to describe the disposition of irinotecan and its primary metabolites SN-38, SN38G, and APC. We have previously reported the use of irinotecan for the treatment of glioma, and described the pharmacokinetics of irinotecan and its metabolites SN-38, and SN38G using non-compartmental approaches [14]. A majority of previous irinotecan pharmacokinetic studies focus on the parent drug and its active metabolite SN-38 [18–20]. Fewer reports studied the pharmacokinetics of its other metabolites SN-38G, NPC and APC.

Xie et al. [21] introduced a multi-compartment model to describe the population pharmacokinetics of irinotecan and its metabolites. The model consisted of one central and two peripheral compartments for the lactone form of irinotecan, a central and a peripheral compartment for the carboxylate form of irinotecan, the lactone form of SN-38, APC, and NPC. The carboxylate form of SN-38 and SN-38G were accounted for using a single compartment and elimination occurring from the central compartments of the carboxylate form of irinotecan, the carboxylate form of SN-38, APC, NPC, and SN-38G. A three compartment model was used to describe the pharmacokinetics of irinotecan in patients with metastatic digestive cancer, while a two compartment model was used for SN-38, and one compartment model was used for SN-38G, APC, and NPC [22]. Ma et al. [23] used a four compartment model to describe the pharmacokinetics of irinotecan, SN-38, and APC in children with recurrent solid tumor using low dose of irinotecan. A altered distribution of SN-38 in two patients was observed suggesting enterohepatic recirculation. None of the above models took into account the phenomena of enterohepatic recirculation.

In order to adequately describe the disposition of irinotecan, the mathematical model should have the capacity to simultaneously describe the pharmacokinetics of irinotecan and its metabolites in the body since the SN-38 metabolite is 1,000-fold more potent than the parent drug

[24], and enzyme induction could affect the formation of the other metabolites APC and NPC. We explored multi-compartment pharmacokinetic models that take into account the enterohepatic recirculation phenomenon. Unlike the model described by Xie et al. [21], the developed model did not take into account the lactone and carboxylate forms of irinotecan and its metabolites since only total drug concentrations were available on our study. Only the lactone form of irinotecan and its metabolites have antitumor activity [25], and they undergo a pH-dependent equilibrium with carboxylate forms [26]. However, the model simultaneously accounts for irinotecan, its metabolites SN-38 and APC, and the phenomena of enterohepatic recirculation.

Pharmacokinetic data from each patient were first evaluated with a model that included irinotecan, SN-38 and APC. After specifying and selectively testing this model, we realized that some of the patients displayed qualitative evidence supporting the enterohepatic recirculation of irinotecan. In a few cases, patients also displayed evidence for the recirculation of SN-38.

Since the combined model did not appear to fit some data sets very well, we decided to formulate a compartmental model that took into account the recirculation phenomenon. After several attempts, we settled on the model depicted in Fig. 2, which consists of the original combined model with a recirculation “chain” added onto the irinotecan compartment. The idea behind this design is that during the infusion, some of the irinotecan added to the primary compartment is channeled into the recirculation chain. After traveling through the chain, it flows back into the irinotecan compartment. Depending on the specifications of the chain, and the total rate at which irinotecan exits the primary compartment, the reflux of irinotecan from the chain can produce a post-infusion increase in the concentration of irinotecan. In particular, the recirculation chain consists of five compartments, each of fixed volume, with a single rate parameter that equal to the rate constant of flow between each compartment in the chain and between the primary compartment and the first chain compartment and the last chain compartment and the primary compartment. The virtue of having a single parameter is that it allows us to model the recirculation effects while adding a minimum of complexity to the model. The number of compartments in the recirculation does not reflect any physiological setting, the five compartments chain provided a model that can best fit the data and does not add much to the complexity of the model.

Several models that account for enterohepatic recirculation of other drugs, using variable number of compartments in the recirculation chain have been published. Three compartments of fixed volume were used to describe the biliary excretion and enterohepatic recirculation of morphine-3-

glucuronide in rats. The recirculation loop was incorporated between the liver compartment and the plasma compartment, and elimination of the drug was assumed to occur partially from the third compartment in the loop [27]. Davis et al. [28] incorporated one compartment to describe the enterohepatic recirculation of gliclazid, however, this compartment was actually considered to be a series of compartments that delay the release of the drug back into the gastrointestinal tract for reabsorption. Enterohepatic recirculation was incorporated as a secondary input to the systemic circulation in describing the population pharmacokinetics of ezetimibe, a single parameter corresponding to the percentage of the dose was incorporated in the model [29]. A bile compartment was used to account for the enterohepatic recirculation of isoflavone biochanin A in rats. The drug was assumed to be transferred directly from the bile compartment to the plasma compartment at regular intervals, and a sine function was used to describe the transfer [30].

After finalizing the form of the recirculation model, we compared it with the standard compartmental model using the criterion of average AIC value. This was calculated in two stages by estimation of parameters for every other patient using both the standard model and the recirculation model. We found that the average AIC value was slightly lower for the set of patients tested using the recirculation model. Having ascertained that the recirculation model yielded reasonable fits for the data, we tested all patients with both models (recirculation and standard).

The best fit model assignment was further confirmed with the good correlation coefficient obtained when comparing the best fit model trapezoidal AUC, calculated from the model output data, with the corresponding actual trapezoidal AUC for each patient (Fig. 4a–c).

In summary, the introduced model can be used to describe the pharmacokinetic of irinotecan and its metabolites following an IV infusion. This model can simultaneously describe the plasma concentration profile of irinotecan and its metabolites when enterohepatic recirculation is present. We have also demonstrated that the standard compartmental model is adequate only when no evidence of enterohepatic recirculation is present. Given the limited number of samples and patients, the intent of this model is to provide a framework or a prototype that takes into account the enterohepatic recirculation phenomenon obtained in some patients and evident by a secondary peak in plasma profile after the end of the infusion. This consideration should be useful for researchers in designing future studies regarding the pharmacokinetic of irinotecan.

Acknowledgments This paper is supported in part by the Mylan Chair of Pharmacology at West Virginia University.

References

1. Clamp AR, Maenpaa J, Cruickshank D, Ledermann J, Wilkinson PM, Welch R, Chan S, Vasey P, Sorbe B, Hindley A, Jayson GC (2006) SCOTROC 2B: feasibility of carboplatin followed by docetaxel or docetaxel-irinotecan as first-line therapy for ovarian cancer. *Br J Cancer* 94(1):55–61
2. Matsumoto K, Katsumata N, Yamanaka Y, Yonemori K, Kohno T, Shimizu C, Andoh M, Fujiwara Y (2006) The safety and efficacy of the weekly dosing of irinotecan for platinum- and taxanes-resistant epithelial ovarian cancer. *Gynecol Oncol* 100(2):412–416
3. Pitot HC, Wender DB, O'Connell MJ, Schroeder G, Goldberg RM, Rubin J, Mailliard JA, Knost JA, Ghosh C, Kirschling RJ, Levitt R, Windschitl HE (1997) Phase II trial of irinotecan in patients with metastatic colorectal carcinoma. *J Clin Oncol* 15(8):2910–2919
4. Conti JA, Kemeny NE, Saltz LB, Huang Y, Tong WP, Chou TC, Sun M, Pulliam S, Gonzalez C (1996) Irinotecan is an active agent in untreated patients with metastatic colorectal cancer. *J Clin Oncol* 14(3):709–715
5. Stupp R, Hegi ME, van den Bent MJ, Mason WP, Weller M, Mirimanoff RO, Cairncross JG (2006) Changing paradigms—an update on the multidisciplinary management of malignant glioma. *Oncologist* 11(2):165–180
6. Slatter JG, Su P, Sams JP, Schaaf LJ, Wienkers LC (1997) Bioactivation of the anticancer agent CPT-11 to SN-38 by human hepatic microsomal carboxylesterases and the in vitro assessment of potential drug interactions. *Drug Metab Dispos* 25(10):1157–1164
7. Humerickhouse R, Lohrbach K, Li L, Bosron WF, Dolan ME (2000) Characterization of CPT-11 hydrolysis by human liver carboxylesterase isoforms hCE-1 and hCE-2. *Cancer Res* 60(5):1189–1192
8. Iyer L, King CD, Whittington PF, Green MD, Roy SK, Tephly TR, Coffman BL, Ratain MJ (1998) Genetic predisposition to the metabolism of irinotecan (CPT-11). Role of uridine diphosphate glucuronosyltransferase isoform 1A1 in the glucuronidation of its active metabolite (SN-38) in human liver microsomes. *J Clin Invest* 101(4):847–854
9. Rivory LP, Robert J (1995) Identification and kinetics of a beta-glucuronide metabolite of SN-38 in human plasma after administration of the camptothecin derivative irinotecan. *Cancer Chemother Pharmacol* 36(2):176–179
10. Catimel G, Chabot GG, Guastalla JP, Dumortier A, Cote C, Engel C, Gouyette A, Mathieu-Boue A, Mahjoubi M, Clavel M (1995) Phase I and pharmacokinetic study of irinotecan (CPT-11) administered daily for three consecutive days every three weeks in patients with advanced solid tumors. *Ann Oncol* 6(2):133–140
11. Canal P, Gay C, Dezeuze A, Douillard JY, Bugat R, Brunet R, Adenis A, Herait P, Lokiec F, Mathieu-Boue A (1996) Pharmacokinetics and pharmacodynamics of irinotecan during a phase II clinical trial in colorectal cancer. *J Clin Oncol* 14(10):2688–2695
12. Santos A, Zanetta S, Cresteil T, Deroussent A, Pein F, Raymond E, Vernillet L, Risse ML, Boige V, Gouyette A, Vassal G (2000) Metabolism of irinotecan (CPT-11) by CYP3A4 and CYP3A5 in humans. *Clin Cancer Res* 6(5):2012–2020
13. Chabot GG (1997) Clinical pharmacokinetics of irinotecan. *Clin Pharmacokinet* 33(4):245–259
14. Friedman HS, Petros WP, Friedman AH, Schaaf LJ, Kerby T, Lawyer J, Parry M, Houghton PJ, Lovell S, Rasheed K, Cloughsey T, Stewart ES, Colvin OM, Provenzale JM, McLendon RE, Bigner DD, Cokgor I, Haglund M, Rich J, Ashley D, Malczyn J, Elfring GL, Miller LL (1999) Irinotecan therapy in adults with recurrent or progressive malignant glioma. *J Clin Oncol* 17(5):1516–1525
15. Chabot GG, Abigeres D, Catimel G, Culine S, de Forni M, Extra JM, Mahjoubi M, Herait P, Armand JP, Bugat R, Clave M, Marty

- ME (1995) Population pharmacokinetics and pharmacodynamics of irinotecan (CPT-11) and active metabolite SN-38 during phase I trials. *Ann Oncol* 6(2):141–151
16. D'Argenio Schumitzky (1997) ADAPT II user's guide: pharmacokinetic/pharmacodynamic systems analysis software. Biomedical Simulations Resource, Los Angeles
 17. Yamaoka K, Nakagawa T, Uno T (1978) Application of Akaike's information criterion (AIC) in the evaluation of linear pharmacokinetic equations. *J Pharmacokinet Biopharm* 6(2):165–175
 18. Azrak RG, Yu J, Pendyala L, Smith PF, Cao S, Li X, Shannon WD, Durrani FA, McLeod HL, Rustum YM (2005) Irinotecan pharmacokinetic and pharmacogenomic alterations induced by methylselenocysteine in human head and neck xenograft tumors. *Mol Cancer Ther* 4(5):843–854
 19. Prados MD, Yung WK, Jaeckle KA, Robins HI, Mehta MP, Fine HA, Wen PY, Cloughesy TF, Chang SM, Nicholas MK, Schiff D, Greenberg HS, Junck L, Fink KL, Hess KR, Kuhn J (2004) Phase I trial of irinotecan (CPT-11) in patients with recurrent malignant glioma: a North American Brain Tumor Consortium study. *Neuro Oncol* 6(1):44–54
 20. Venook AP, Enders KC, Fleming G, Hollis D, Leichman CG, Hohl R, Byrd J, Budman D, Villalona M, Marshall J, Rosner GL, Ramirez J, Kastrissios H, Ratain MJ (2003) A phase I and pharmacokinetic study of irinotecan in patients with hepatic or renal dysfunction or with prior pelvic radiation: CALGB 9863. *Ann Oncol* 14(12):1783–1790
 21. Xie R, Mathijssen RH, Sparreboom A, Verweij J, Karlsson MO (2002) Clinical pharmacokinetics of irinotecan and its metabolites in relation with diarrhea. *Clin Pharmacol Ther* 72(3):265–275
 22. Poujol S, Bressolle F, Duffour J, Abderrahim AG, Astre C, Ychou M, Pinguet F (2006) Pharmacokinetics and pharmacodynamics of irinotecan and its metabolites from plasma and saliva data in patients with metastatic digestive cancer receiving Folfiri regimen. *Cancer Chemother Pharmacol* 58(3):292–305
 23. Ma MK, Zamboni WC, Radomski KM, Furman WL, Santana VM, Houghton PJ, Hanna SK, Smith AK, Stewart CF (2000) Pharmacokinetics of irinotecan and its metabolites SN-38 and APC in children with recurrent solid tumors after protracted low-dose irinotecan. *Clin Cancer Res* 6(3):813–819
 24. Kawato Y, Aonuma M, Hirota Y, Kuga H, Sato K (1991) Intracellular roles of SN-38, a metabolite of the camptothecin derivative CPT-11, in the antitumor effect of CPT-11. *Cancer Res* 51(16):4187–4191
 25. Hertzberg RP, Caranfa MJ, Holden KG, Jakas DR, Gallagher G, Mattern MR, Mong SM, Bartus JO, Johnson RK, Kingsbury WD (1989) Modification of the hydroxy lactone ring of camptothecin: inhibition of mammalian topoisomerase I and biological activity. *J Med Chem* 32(3):715–720
 26. Fassberg J, Stella VJ (1992) A kinetic and mechanistic study of the hydrolysis of camptothecin and some analogues. *J Pharm Sci* 81(7):676–684
 27. Ouellet DM, Pollack GM (1995) Biliary excretion and enterohepatic recirculation of morphine-3-glucuronide in rats. *Drug Metab Dispos* 23(4):478–484
 28. Davis TM, Daly F, Walsh JP, Ilett KF, Beilby JP, Dusci LJ, Barrett PH (2000) Pharmacokinetics and pharmacodynamics of gliclazide in Caucasians and Australian Aborigines with type 2 diabetes. *Br J Clin Pharmacol* 49(3):223–230
 29. Ezzet F, Krishna G, Wexler DB, Statkevich P, Kosoglou T, Batra VK (2001) A population pharmacokinetic model that describes multiple peaks due to enterohepatic recirculation of ezetimibe. *Clin Ther* 23(6):871–885
 30. Moon YJ, Sagawa K, Frederick K, Zhang S, Morris ME (2006) Pharmacokinetics and bioavailability of the isoflavone biochanin A in rats. *AAPS J* 8(3):E433–E442